

Follow-Up Research of Transiting Exoplanet Candidates Sophie Welsh

Abstract

In this project, the goal was to perform follow-up spectroscopy on transiting exoplanet candidates and confirm or reject their status as bona fide planets. The original photometric data were provided by the K2 mission and initially processed by Andrew Vanderburg, who then gave us several target names to narrow down. We followed a subset of these targets through the observation period, particularly EP202093968, chosen for the promise it showed early in the observations. We then analyzed the light curve solutions and results from the spectra and found that all of them were false positives. Although the data in this case did not confirm a planetary system, we used the same methods and processes we would have used in planetary cases. Our mass and radius determination for the late M dwarf companion of EP202093968 is significant in testing models for the structure of cool dwarfs. The analysis yielded a primary mass and radius of $1.244 \pm 0.086 M_{\text{Sun}}$ and $1.51 \pm 0.28 R_{\text{Sun}}$, and a secondary mass and radius of $0.146 M_{\text{Sun}}$ and $0.201 \pm 0.037 R_{\text{Sun}}$.

On K2 and TRES

This project utilizes data from the K2 mission, which was initiated after two of the four reaction wheels for the original Kepler mission failed. For four years, the photometer on the original mission provided light curve data in a search for transiting planets in a single target field on the sky, maintaining its orientation toward that area using three reaction wheels. Light curves from measurements over the course of a planet's transit, combined with the orbital inclination, give an estimate for the planet's radius from the amount of light blocked. In edge-on systems as in the cases of the targets observed in this report, the inclination is such that the secondary passes directly in front of the primary, facilitating the determination of relative ratios of the objects' radii (from the proportion of flux blocked, which is correlated with area). These results, in conjunction with other methods of study, give a glimpse of the planet's properties. In particular, using spectroscopy to track the radial velocity measurements for a host star allows to infer a mass for the planet. Combining the mass and radius allows us to infer the planet's surface gravity and density, and thus to judge whether it is a gas giant, water world, or rocky planet.

However, after the Kepler mission lost two reaction wheels (including the spare), it became impossible for the mission to continue its original mission and in the same manner. Consequently, the mission was repurposed and renamed "K2", and rather than using three wheels to keep itself oriented in one direction, as Kepler did, it uses two reaction wheels plus photon pressure from the Sun and thruster firings to keep itself balanced in the ecliptic. Its thrusters can also redirect it to a new field of view. Rocky and Earth-like planets are of particular interest, particularly the mass-radius relation for small planets in the range of rocky planets and small Neptunes (whose sizes fall between those of Earth and Neptune and which dominate the galactic census).

Kepler observed a single area on the sky, but with the repurposing into K2 the observed area of the sky has been broadened (though restricted to the ecliptic), the observing time divided into 83-day segments, or "campaigns", and number of targets

increased by more than 100,000 stars, focusing on nearby bright stars and M dwarfs. For this project, the photometric data came from Campaign Zero. My role was in assisting with follow-up work in order to filter out irrelevant target objects, such as false positives due to eclipsing binaries rather than planets while retaining the most “interesting” and potentially useful confirmed candidates for further investigation.

In addition to photometric data from K2, we were very fortunate to have access to telescope time on the Tillinghast Reflector Echelle Spectrograph (TRES) at the Fred Lawrence Whipple Observatory, for two or three weeks each month.

Methodology and Initial Photometry

The general methodology for transiting exoplanet candidate identification and confirmation consists of a number of steps, including photometric and spectroscopic follow-up processes. The initial data for my project consisted of photometric data from the K2 mission’s Campaign Zero. This gave the ephemeris of each candidate’s orbit, consisting of the transit’s period and a reference epoch for the time of one of the transits. The K2 photometric data gave a light curve, for which I made a solution by using a program known as EXOFAST. But because photometry alone can only give the radius of the secondary as a proportion of the primary, spectroscopic follow-up becomes necessary in order to estimate the relative masses as well as provide stellar parameters for the primary.

Spectroscopic data are crucial in yielding certain variables pertaining to the objects -- namely, metallicity, surface gravity, and effective temperature – which we match up to existing models of stellar types to find the best fit for the primary. From there we can guess the average mass and radius values for a star of that type, from which we infer the corresponding values for the secondary. As a final step, we use these obtained mass and radius values to analyze the system and attempt an interpretation to confirm or reject the secondary as a false positive.

The processes for both photometric and spectroscopic follow-up will be described in further detail below, presented with the actual data.

Table 1: Initially known values for EP202093968

Target name	Coordinates	Tc (BJD)	Period (days)	Apparent Magnitude (V)	J-K Color	Number of observations
EP202093968	06:24:38.70 21:07:32.70	2454835.42557500	2.4701215800	10.2	0.21	15

The following figure shows the initial photometric data for candidate EP202093968.

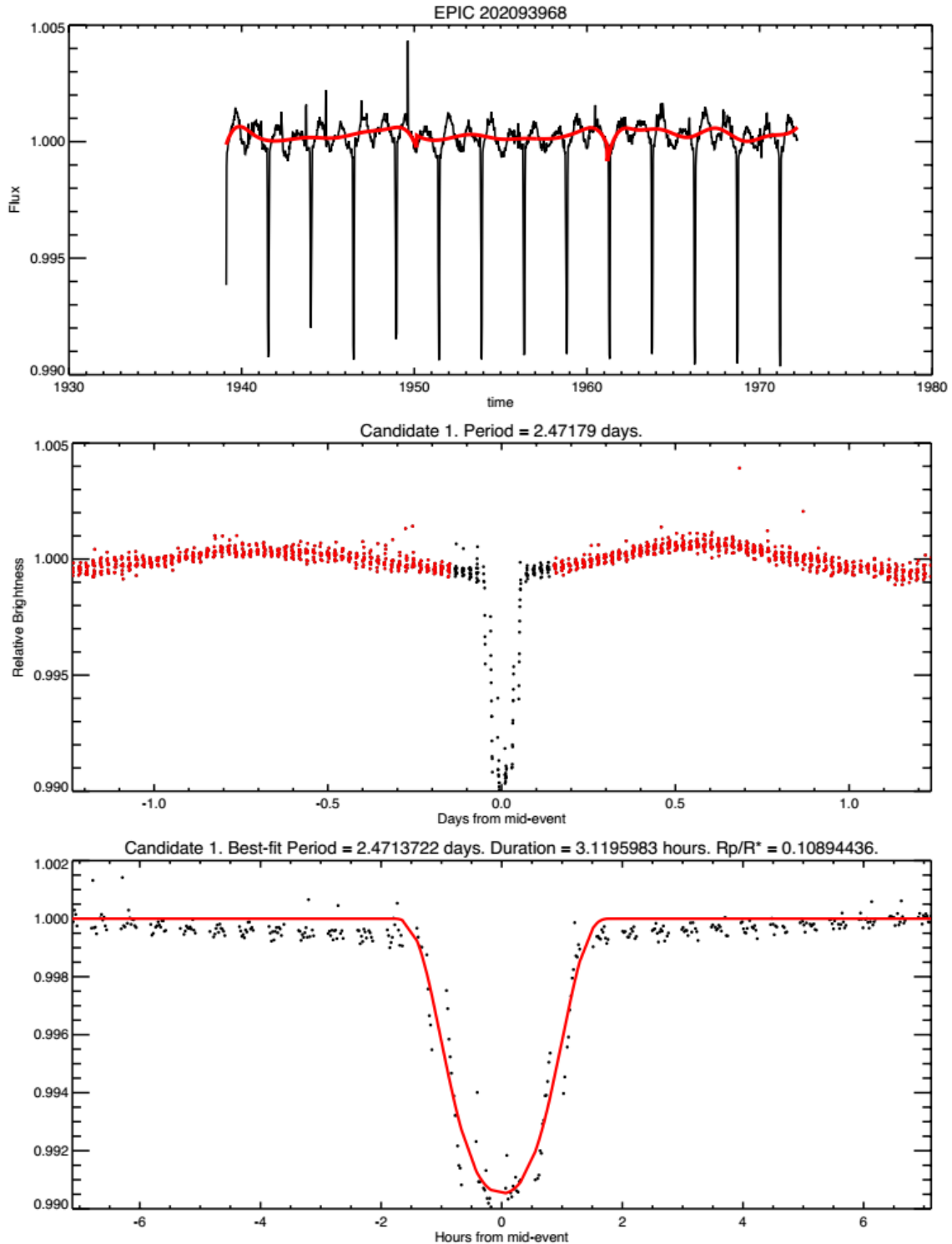


Fig. 1: K2 photometric data for EP2020939368. The fluctuations in the top panel are due to ellipsoidal variations. Due to the strong gravitational interaction between the objects in the system, they are distorted, causing regular variations in flux as their apparent sizes change during their orbit.

In addition, we see some of the ellipsoidal-induced variations being alternately greater than others due to a Doppler beaming effect, which increases the apparent luminosity of an object

moving toward the observer along the line of sight. Though the best way to account for this would have been to run a “BEER” analysis, which is described in Faigler et al. (2012), it was not possible to learn and perform this analysis within the time constraints.

Spectroscopy

Andrew Vanderburg, a collaborator, gave us three sets of K2 targets which he had identified from a much larger set as having a sufficiently high probability of being a planetary system that they were worth following up. I learned to make a .nam file, which basically served as an observing plan for TRES, and organized some information in the file after some trivial conversions of the RA and DEC of each star from degrees to sexagesimal coordinates. We also assigned a priority level to each target, depending on the practical feasibility of observing each target as well as the perceived likelihood of confirming each target based on the data we had.

The plan for the K2 targets were then merged into the queue observing plan to be observed over the course of several weeks with TRES, run by a team of remote observers (Gilbert Esquerdo, Perry Berlind, and Mike Calkins).

In particular, we decided to observe EP202093968 each night on which conditions allowed observation and to focus on this star for this project. Our earliest observations had already shown that there was a stellar companion, most likely a low-mass M dwarf. Although we knew that the companion was not planetary, the equations we would use to solve for the companion’s parameters in the case of a planetary companion are the same as what we have shown below.

The fifteen spectroscopic observations gave results which we compiled into an orbital solution, and combined with the light curve solution from the photometric observation, EXOFAST gave outputs for important parameters including the mass and radius of the secondary.

EP202093968, 06:24:38.70 21:07:32.70, V=10.2, PM=26.6, J-K=0.21, Period=2.5

2014-11-07 TRES, pha=863.72, RV=-0.266, Teff=6500+/-125, log(g)=4.00+/-0.25, Vrot=35.0+/-2.0, [m/H]=0.00+/-0.25, ccf=0.924, SNRe=34.4, R=m
--

2014-11-08 TRES, pha=864.04, RV=-21.956, Teff=6750+/-125, log(g)=4.50+/-0.25, Vrot=25.0+/-2.0, [m/H]=0.00+/-0.25, ccf=0.931, SNRe=37.6, R=m

2014-11-13 TRES, pha=866.15, RV=-32.919, Teff=6500+/-125, log(g)=4.00+/-0.25, Vrot=30.0+/-2.0, [m/H]=0.00+/-0.25, ccf=0.953, SNRe=50.8, R=m

2014-11-15 TRES, pha=866.97, RV=-14.088, Teff=6750+/-125, log(g)=4.50+/-0.25, Vrot=25.0+/-2.0, [m/H]=0.00+/-0.25, ccf=0.958, SNRe=50.3, R=m

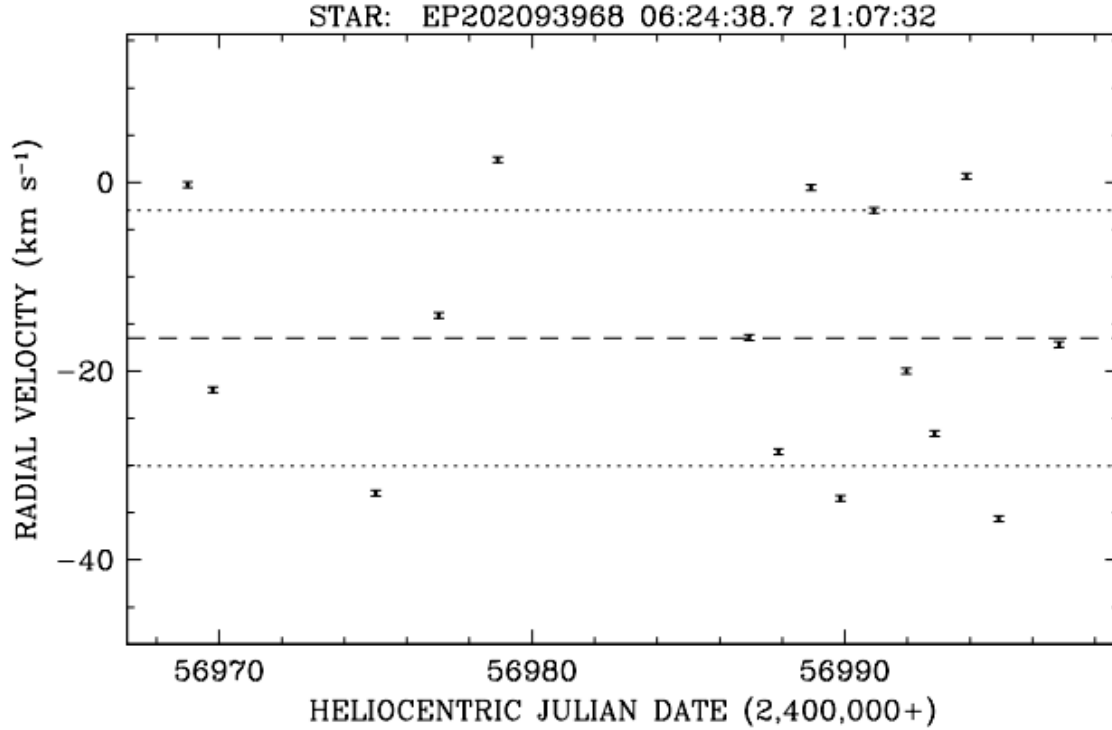
2014-11-17 TRES, pha=867.73, RV=2.387, Teff=6500+/-125, log(g)=4.00+/-0.25, Vrot=30.0+/-2.0, [m/H]=0.00+/-0.25, ccf=0.973, SNRe=63.2, R=m

2014-11-25 TRES, pha=870.98, RV=-16.419, Teff=6250+/-125, log(g)=4.00+/-0.25, Vrot=25.0+/-2.0, [m/H]=0.00+/-0.25, ccf=0.937, SNRe=42.9, R=m
2014-11-26 TRES, pha=871.36, RV=-28.521, Teff=7000+/-125, log(g)=4.50+/-0.25, Vrot=30.0+/-2.0, [m/H]=0.00+/-0.25, ccf=0.960, SNRe=60.4, R=m
2014-11-27 TRES, pha=871.78, RV=-0.526, Teff=6500+/-125, log(g)=4.00+/-0.25, Vrot=30.0+/-2.0, [m/H]=0.00+/-0.25, ccf=0.937, SNRe=46.2, R=m
2014-11-28 TRES, pha=872.16, RV=-33.452, Teff=7000+/-125, log(g)=4.50+/-0.25, Vrot=35.0+/-2.0, [m/H]=0.00+/-0.25, ccf=0.969, SNRe=63.6, R=m
2014-11-29 TRES, pha=872.60, RV=-2.951, Teff=7000+/-125, log(g)=4.50+/-0.25, Vrot=30.0+/-2.0, [m/H]=0.00+/-0.25, ccf=0.968, SNRe=60.6, R=m
2014-11-30 TRES, pha=873.02, RV=-19.688, Teff=6750+/-125, log(g)=4.50+/-0.25, Vrot=25.0+/-2.0, [m/H]=0.00+/-0.25, ccf=0.959, SNRe=54.7, R=m
2014-12-01 TRES, pha=873.38, RV=-26.625, Teff=6500+/-125, log(g)=4.00+/-0.25, Vrot=30.0+/-2.0, [m/H]=0.00+/-0.25, ccf=0.968, SNRe=59.3, R=m
2014-12-02 TRES, pha=873.79, RV=0.657, Teff=7000+/-125, log(g)=4.50+/-0.25, Vrot=30.0+/-2.0, [m/H]=0.00+/-0.25, ccf=0.959, SNRe=50.9, R=m
2014-12-03 TRES, pha=874.21, RV=-35.638, Teff=4750+/-125, log(g)=2.50+/-0.25, Vrot=35.0+/-2.0, [m/H]=0.00+/-0.25, ccf=0.761, SNRe=33.8, R=m
2014-12-05 TRES, pha=874.99, RV=-17.198, Teff=7000+/-125, log(g)=4.50+/-0.25, Vrot=30.0+/-2.0, [m/H]=0.00+/-0.25, ccf=0.985, SNRe=107.7, R=m

Table 2: Log of TRES Observations and Quick-Look Parameters Obtained for Candidate EP202093968

There are some anomalous points in the data. First, we see that the observation on the fifth night seems to have been contaminated by moonlight; the stellar parameter values yielded by data taken on this night alone differ drastically from those given by other observations. However, it appears that the radial velocity was not affected, so we have left it in our analysis. In addition, there are some observations (those clustered around phase 0.4~06) with larger residuals than the rest of the observations, as can be seen in the orbital phase plot (see Fig. 3). This scatter remains unexplained; it may be due to contamination by the light of a **nearby star** that varied with the image quality.

Fig. 2: Radial velocity history for EP202093968

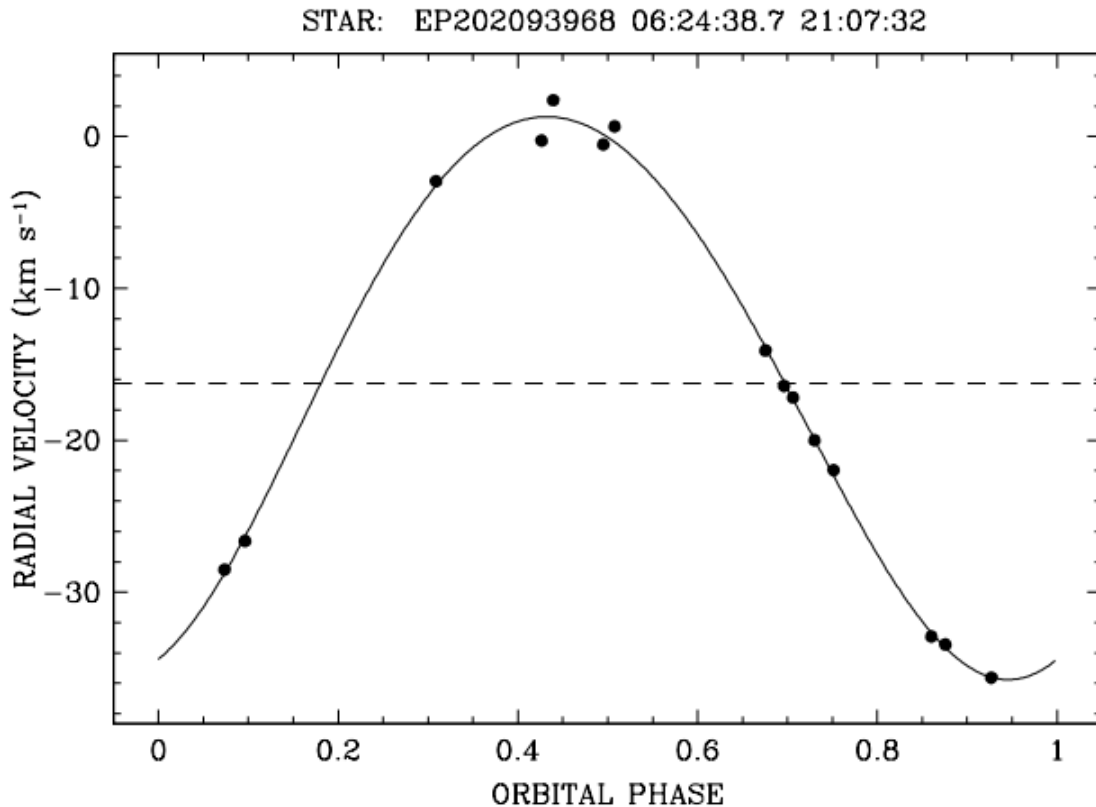


These velocities can then be reorganized by phase and expressed in terms of their place in the orbit.

Fig. 3: Orbital phase plot for EP202093968.

There is a puzzling trend here: though most of the points fall cleanly on the fit curve, those close to phase 0.4 have more scatter. We are unsure what could have caused the residuals to appear

here.



Because the time constraints of this project were prohibitive of more involved forms of analysis, such as those using PHOEBE or BEER analysis to create light curve solutions I used a program known as EXOFAST. In this case, EXOFAST required that I enter a number of parameters obtained from spectroscopic data – namely, metallicity, effective temperature, surface gravity, and ephemeris, as well as errors for each parameter. Allyson Bieryla, a collaborator in the group, ran a code known as Spectral Parameter Classification on the target spectra in order that I could enter reliable stellar parameters into EXOFAST. Whereas the quick-look parameters shown in Table 2 assume a solar metallicity for the primary, SPC allows the metallicity to float as a free parameter, and the spectrum is cross correlated with a library of parameters from synthetic spectra to find a best fit. After SPC derived the values shown in Table 3, I then took the mean values for each parameter, and the results were as follows:

Table 3: Parameters obtained from SPC, with inflated error values necessary in order to obtain an accurate mass value for the primary

	Mean value	Standard error	Inflated error
T_{eff}	6515.4507	33.57160978	100
Log(g)	4.0908	0.057073134	0.10
[m/H]	-0.1156	0.039884547	0.08

These values represent, respectively, the effective temperature, log of surface gravity, and metallicity as given by TRES observations, and along with the inflated errors, they were fed into EXOFAST to produce the light curve solution, which is presented below.

We did not include the observation from the fifth night due to a low signal-to-noise ratio and the strong skew in the values as a result.

The following is the output obtained from EXOFAST, with the help of Jason Eastman, who developed the program.

```
WARNING: results will not be reliable unless transit data spans
multiple periods; Enter prior width on period to remove this error.
Click here for an explanation of the outputs.
/usr/local/itt/idl64/bin/idl -e "in = 9d999 & exofast,
tranpath='/var/tmp/2v7ylb5cvnsmjmim3c.flux',priors =
transpose([[0d0,0d0,2454835.42557500d0,0.39273489522538d0,0d0,0d0,0d0,0
d0,0d0,0d0,4.0908d0,6515.4507d0,-
0.1156d0,0d0,0d0,0d0,0d0,0d0,0d0],[in,in,in,in,in,in,in,in,in,in,0.10d0
,100d0,0.08d0,in,in,in,in,in,in]),/longcadence,/noslope,/circular,band
='Kepler',/bestonly,prefix='/var/tmp/2v7ylb5cvnsmjmim3c.'"
```

```
Transit fit:
Chi^2/dof = 1.42
Scaling errors by 1.19
RMS of residuals = 0.00029
```

```
Combined fit: Chi^2 of Transit data = 269.4 (288 data points)
Chi^2 of Priors = 0.00171 (3 priors)
Chi^2/dof = 0.972
```

Stellar Parameters:

M_{*}	Mass (\msun)	1.36
R_{*}	Radius (\rsun)	1.75
L_{*}	Luminosity (\lsun)	4.95
\rho_{*}	Density (cgs)	0.36
\log(g_{*})	Surface gravity (cgs)	4.09
\teff	Effective temperature (K)	6515.56
\feh	Metallicity	-0.12

Planetary Parameters:

P	Period (days)	2.47
a	Semi-major axis (AU)	0.040
R_{P}	Radius (\rj)	1.73
T_{eq}	Equilibrium Temperature (K)	2086.90
\fave	Incident flux (\fluxcgs)	4.30

Primary Transit Parameters:

T_C	Time of transit (\bjdtdb)	2454835.561006
R_{P}/R_{*}	Radius of planet in stellar radii	0.10
a/R_{*}	Semi-major axis in stellar radii	4.87
u_1	linear limb-darkening coeff	0.29
u_2	quadratic limb-darkening coeff	0.31
i	Inclination (degrees)	79.98
b	Impact Parameter	0.847925
\delta	Transit depth	0.010
T_{FWHM}	FWHM duration (days)	0.082
\tau	Ingress/egress duration (days)	0.033
T_{14}	Total duration (days)	0.12
P_{T}	A priori non-grazing transit prob	0.18

$P_{\{T,G\}}$	A priori transit prob	0.23
F_0	Baseline flux	1.000074

Secondary Eclipse Parameters:

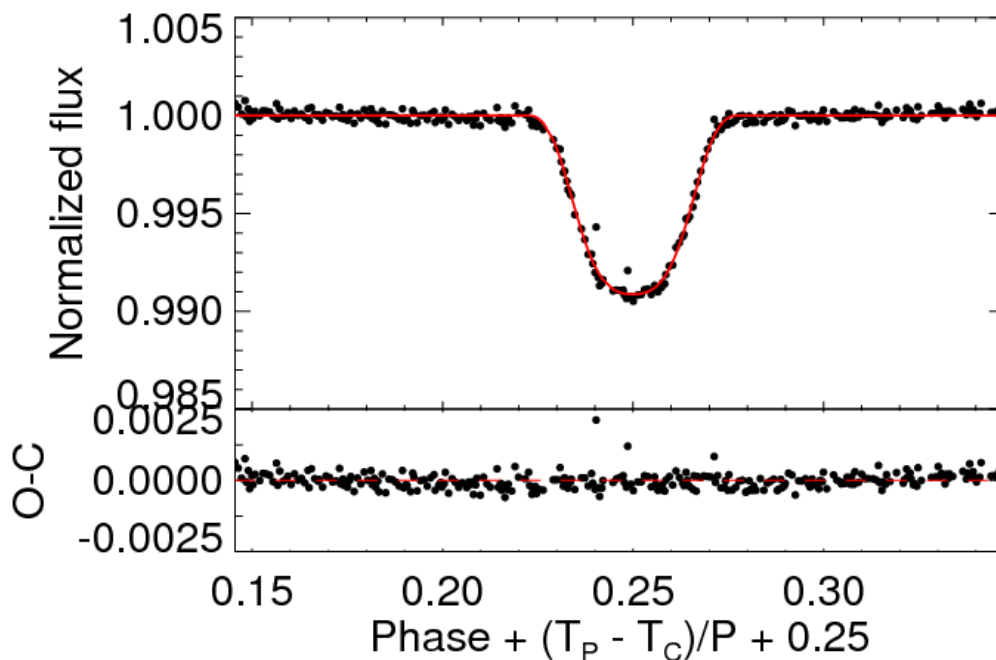
$T_{\{S\}}$	Time of eclipse (\backslash bjdtdb)	2454836.796028
-------------	--	----------------

Errors from Carter et al., 2008 (eqs 19 & 23):

\backslash sigma_{\{T,C\}}	\sim 0.00016818076	\backslash sigma_{\{\tau\}}	\sim 0.00058
\backslash sigma_{\{T,FWHM\}}	\sim 0.00033636152	\backslash sigma_{\{\text{depth}\}}	\sim 4.67e-05

NOTE: depth used here (0.010290907) is not delta
if the transit is grazing

NOTE: If chi2/dof of combined fit is not \sim 1, do not trust these --
rerun with errors equal to your original errors multiplied by the
scaling



[Transit Model](#)

Judging from the tight fit of the light curve produced by EXOFAST, unlike the photometric plots shown in Figure 1, it seems that the program may correct for ellipsoidal variations.

One method to derive the mass and radius of the primary is to run a Markov Chain Monte Carlo analysis, which I did not have the time or experience to do in this project and which was kindly provided by Guillermo Torres. The procedure required, again the stellar parameter values given in Table 3 (effective temperature, surface gravity, and metallicity, with errors). The analysis yielded the following results for the primary star:

Mass = $1.244 \pm 0.086 M_{\text{Sun}}$ (compare to the value of 1.36 estimated for EXOFAST analysis)

Radius = $1.51 \pm 0.28 R_{\text{Sun}}$ (compare to the value of 1.75 assumed in EXOFAST analysis)

Age = 2.8 ± 1.0 Gyr

The aperture used for the K2 photometry is not clear of other stars, so we have to account for the resulting contamination in calculating the stellar radius by dividing by a dilution factor. We corrected for the effect of the extraneous flux (from a star 1.2 magnitudes fainter) by dividing by a dilution factor of $1/1.33 = 0.75$.

This gives a final radius value of $1.51/0.75 = 2.013$ (using the result from MCMC).

We derive the mass and radius of the secondary object using the result from MCMC analysis: using that $R_p/R^* = 0.1$ (from the EXOFAST light curve solution), we find that $R_2 = 1.51/0.75 = 0.201 \pm 0.037$ (though this really depends on the error in the primary mass).

To find the secondary mass, we can solve the equation:

$$M_2 \sin(i) = 0.1174 (M_1 + M_2)^{2/3} M_{\text{Sun}}$$

with known value for M_1

After solving iteratively, I found $M_2 = 0.146 M_{\text{Sun}}$

As a result, we can guess that the secondary is an M dwarf.

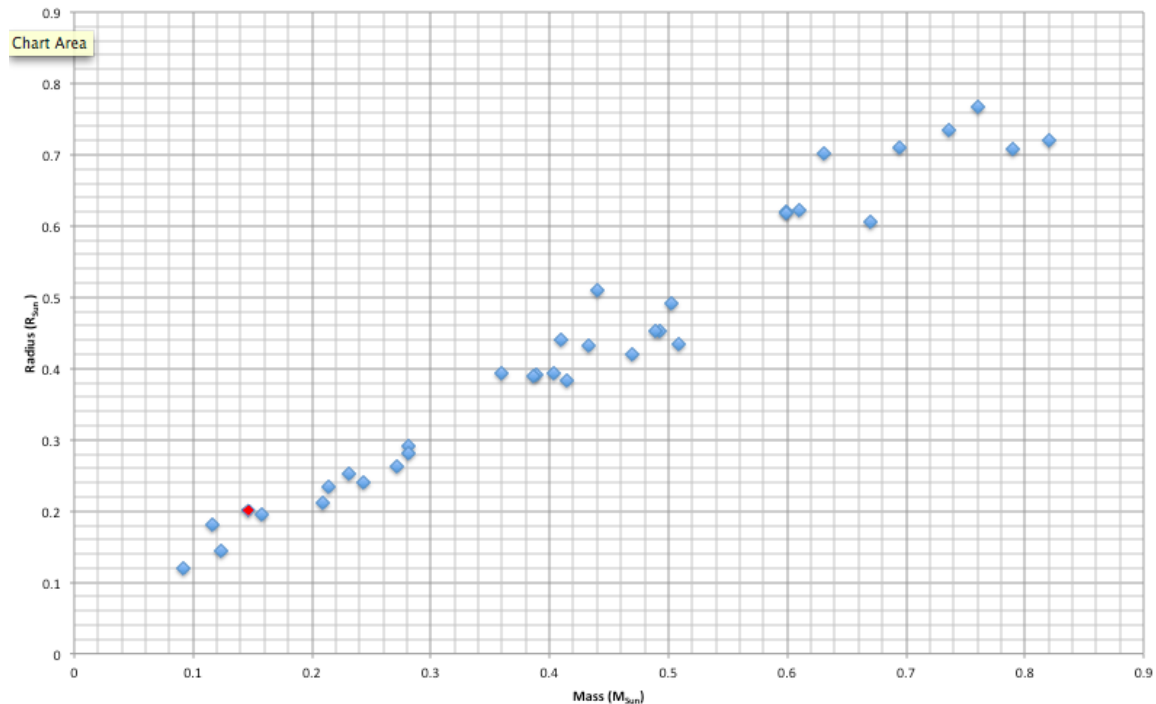


Fig. 4: Mass-radius diagram for a sample of low-mass stars (points obtained from Ribas 2005). The secondary object of the EP202093968 system is included here in red.

Other Targets Observed

First, a note on reading the spectra:

The following figure shows an example of part of the data layout provided by TRES, including a typical result for a clean spectrum with prominent magnesium b lines.

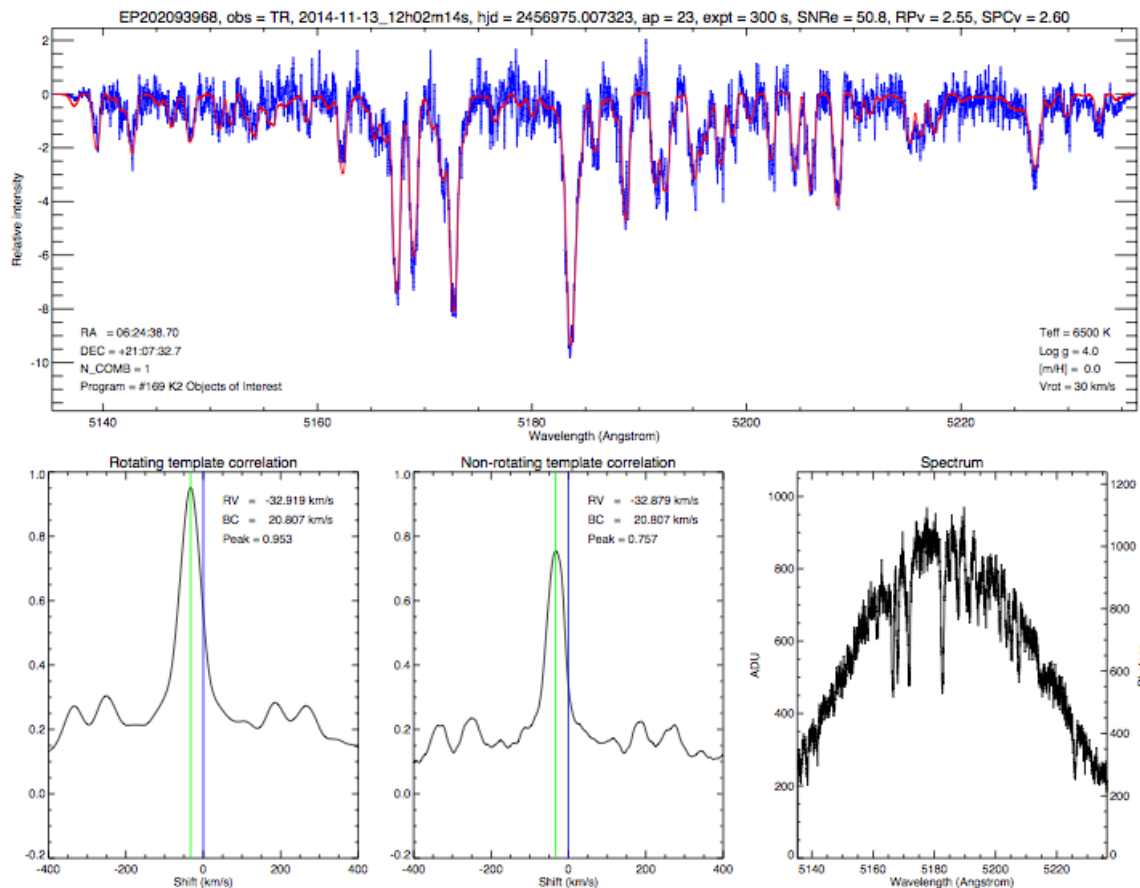


Fig. 4: Spectrum and cross correlation functions from one TRES observation of EP202093968 (taken on 13 November 2014)

The two components of the greatest interest here are the top panel, showing the spectrum itself, and the “non-rotating” cross correlation function directly below the spectrum and in the middle. An examination of the correlation function peak can reveal important information: “bumps” which make the central peak asymmetrical point to the velocities of various components of the observed target.

Table 4: Initially known values for other target candidates followed up with TRES

Target name	Coordinates	Tc (BJD)	Period (days)	Apparent Magnitude (V)	J-K Color	Number of observations
EP202091388	06:05:27.31 21:15:21.70	2454836.98705900	6.476266900	13.5	0.398	2
EP202088	06:22:33	2454833.87218	2.6195056	11.6	0.32	2

212	.90 14:44:30 .40	400	00			
EP202092 782	06:10:26 .99 16:51:54 .80	2454845.75925 000	13.336104 000	11.6	0.21	3
EP202094 740	06:41:51 .15 27:05:50 .00	2454833.00905 600	0.6896972 90	11.5	0.24	3
EP202090 723	06:00:54 .83 23:56:18 .90	2454834.81979 200	6.1482573 00	11	0.27	3
EP202089 657	06:05:48 .85 23:29:04 .30	2454833.41497 400	1.3148192 00	11.6	0.31 1	2
EP202087 156	06:24:07 .07 14:46:17 .30	2454833.48001 700	0.9472926 10	12.3	0.27 2	3

The following is a summary of the results for each target, accompanied by a list of quick-look parameters obtained from the spectroscopic observations (including RA, DEC, proper motions, J-K color, period, phase, radial velocity, effective temperature, log(surface gravity), rotational velocity, metallicity, and peak value for the correlation function, and signal to noise ratio per resolution element).

EP202091388

EP202091388, 06:05:27.31 21:15:21.70, V=13.5, PM=7.0, J-K=0.40, Period=6.5

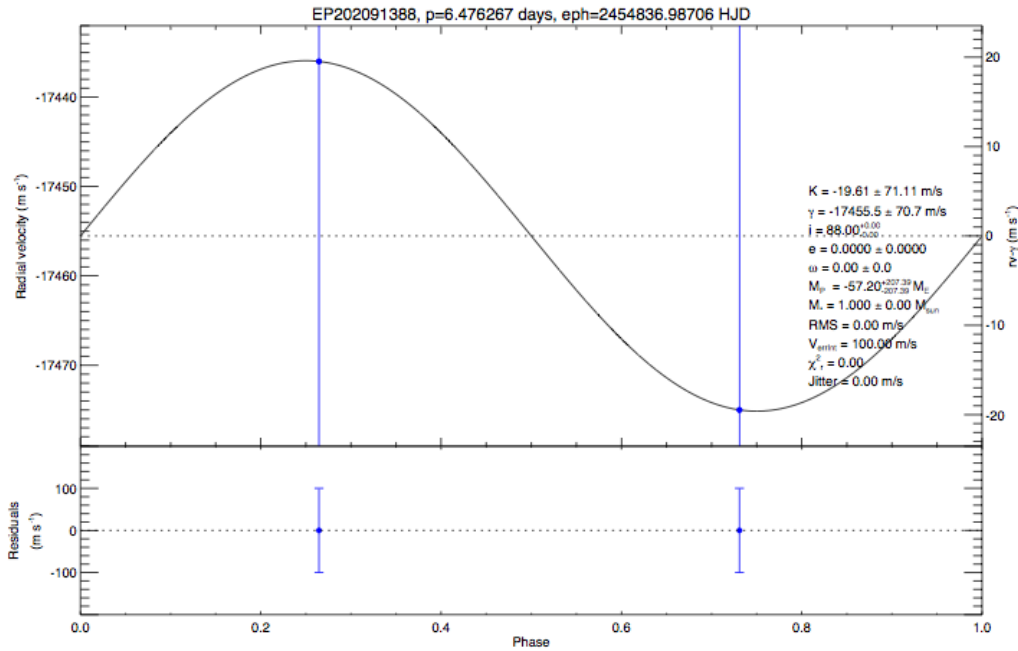
2014-11-17 TRES, pha=330.73, RV=-17.475, T_{eff}=5500+/-125, log(g)=4.50+/-0.25, V_{rot}=6.0+/-2.0, [m/H]=0.00+/-0.25, ccf=0.962, SNRe=28.6, R=m

2014-11-27 TRES, pha=332.26, RV=-17.436, T_{eff}=5750+/-125, log(g)=4.50+/-0.25, V_{rot}=6.0+/-2.0, [m/H]=0.00+/-0.25, ccf=0.955, SNRe=26.6, R=m

The first observation taken on the 17th of November was clean and promising, so we took another observation on the 26th, when the phase was at the opposite quadrature (near 0.25).

The second observation showed a negligible radial velocity change and similarly a negligible change in the correlation function shape. However, the radial velocity is out of phase with the ephemeris, as the phase plot shows (going down rather than up near phase zero), resulting in a calculated mass for the secondary which is a negative value as

shown on the phase plot. The reason for this is unknown; one possibility is an inaccurate photometric ephemeris (error in determining the phase). Another likely explanation is errors in the velocities larger than the true variation.



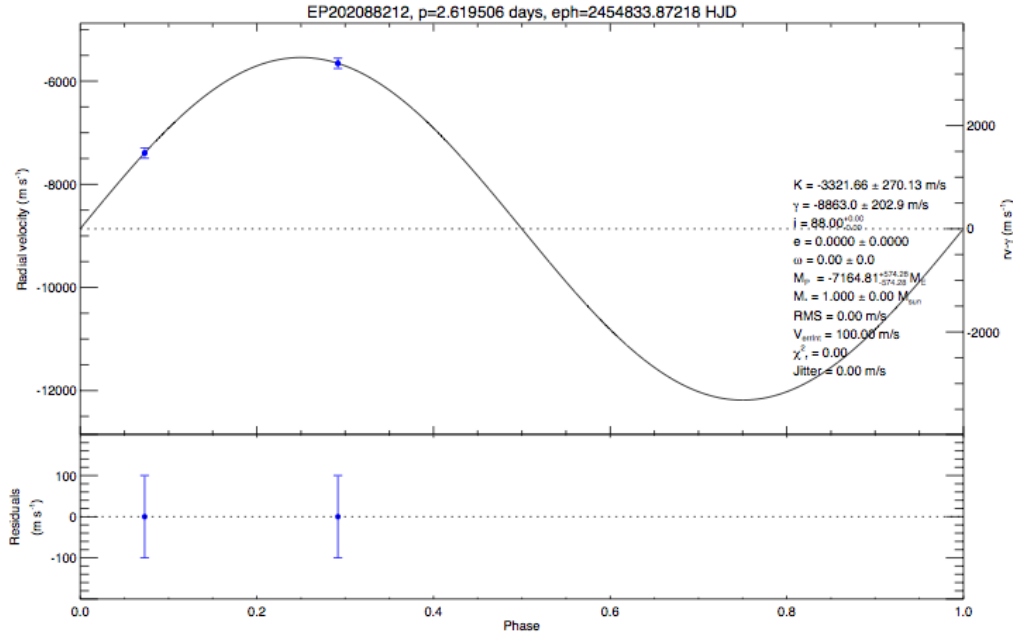
EP202088212

EP202088212, 06:22:33.90 14:44:30.40, V=11.6, PM=5.6, J-K=0.32, Period=2.6

2014-11-07 TRES, pha=815.07, RV=-7.394, T_{eff}=6250+/-125, log(g)=4.50+/-0.25, V_{rot}=12.0+/-2.0, [m/H]=0.00+/-0.25, ccf=0.933, SNRe=32.3, R=m

2014-11-26 TRES, pha=822.29, RV=-5.655, T_{eff}=6250+/-125, log(g)=4.50+/-0.25, V_{rot}=12.0+/-2.0, [m/H]=0.00+/-0.25, ccf=0.932, SNRe=34.3, R=m

For the first observation, the phase was about zero, and there was a very slight bulge on the left side of the correlation function. We planned to observe it again near either quadrature (phase at 0.25 or 0.75), predicting that there would be a companion. We saw a velocity change of 2km/s which was again out of phase with the photometric ephemeris.

**EP202092782**

EP202092782, 06:10:26.99 16:51:54.80, V=11.6, PM=6.9, J-K=0.21,
 Period=13.3

2014-11-07 TRES, pha=159.20, RV=1.486, Teff=5750+/-125,
 log(g)=2.00+/-0.25, Vrot=35.0+/-2.0, [m/H]=0.00+/-0.25,
 ccf=0.675, SNRe=34.0, R=m

2014-11-15 TRES, pha=159.81, RV=18.284, Teff=9250+/-125,
 log(g)=3.00+/-0.25, Vrot=20.0+/-2.0, [m/H]=0.00+/-0.25,
 ccf=0.682, SNRe=32.1, R=m

2014-11-27 TRES, pha=160.70, RV=15.389, Teff=9750+/-125,
 log(g)=3.50+/-0.25, Vrot=20.0+/-2.0, [m/H]=0.00+/-0.25,
 ccf=0.775, SNRe=46.7, R=m

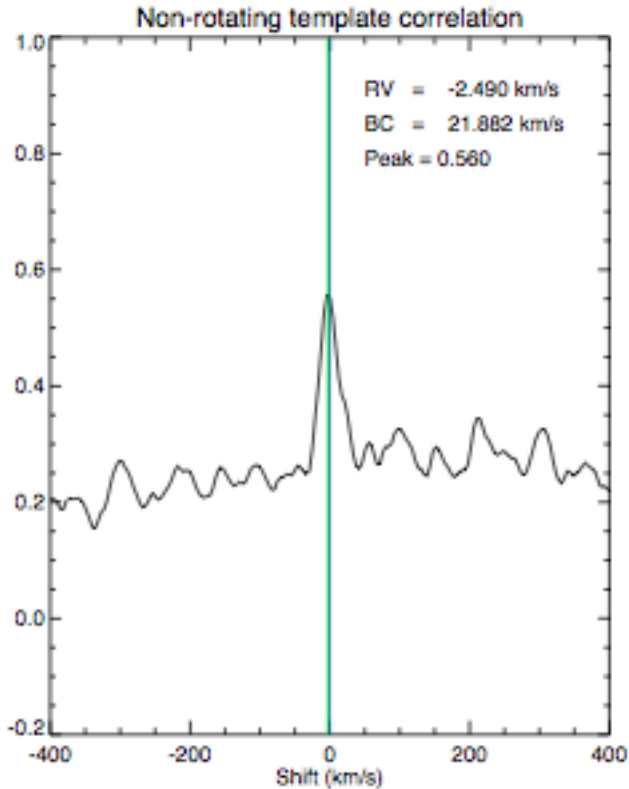
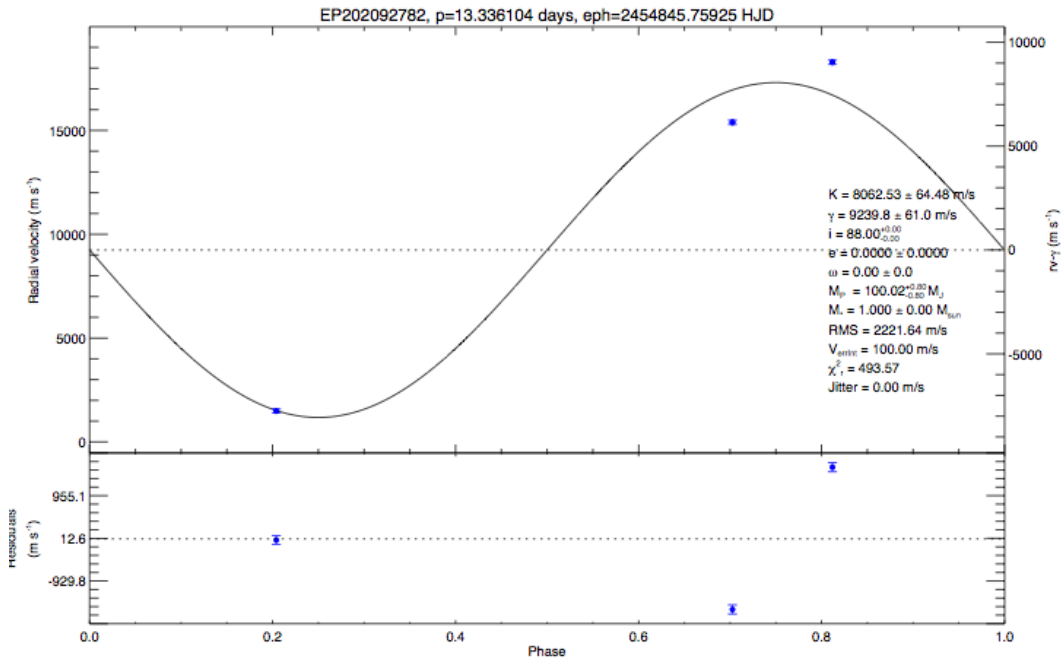


Fig. Correlation function of EP202092782 on the first observation night

On the first night we tentatively noted a very slight bump on the right side of the correlation function. It was a mystifying pattern, with shallow lines. There seems to be a nontrivial degree of contamination from scattered moonlight, due to the fact that the target was 48 degrees from the moon on the first observation night. We see evidence of this contamination in the facts that the correlation function bulges at the expected lunar velocity and that the spectrum reveals composite data pulled toward solar values. In order to make sure that this effect is not the result of a stellar companion in the vicinity of the target, we took another observation near phase 0.75 and obtained a much cleaner spectrum as well as parameter values which were very different from what we saw on the first night. The jump in radial velocity was particularly noteworthy, and the high temperature was inconsistent with the slow rotation and narrow lines if interpreted as the result of a reddened A star. We took one more observation as a result.

The third observation yielded parameters which were much closer to those seen on the second night than those from the first, including effective temperature, radial velocity, surface gravity, and rotational velocity. We ascribe the differences between the results from the first night and those from the second and third nights to the strong factor of scattered moonlight on the first night. However, if we look at the phase plot with the contaminated first observation excluded, the result is a phase plot out of phase with the photometric ephemeris, and we requested to observe it again near phase 0.25 for a clearer picture of what is happening in the system.



EP202094740

EP202094740, 06:41:51.15 27:05:50.00, V=11.5, PM=2.2, J-K=0.24, Period=0.7

2014-11-07 TRES, pha=3097.01, RV=-10.833, Teff=6500+/-125, log(g)=3.50+/-0.25, Vrot=80.0+/-2.0, [m/H]=0.00+/-0.25, ccf=0.870, SNRe=35.3, R=m

2014-11-27 TRES, pha=3125.79, RV=-11.979, Teff=5750+/-125, log(g)=3.00+/-0.25, Vrot=110.0+/-2.0, [m/H]=0.00+/-0.25, ccf=0.857, SNRe=31.7, R=m

2014-11-28 TRES, pha=3127.23, RV=-14.026, Teff=6000+/-125, log(g)=3.00+/-0.25, Vrot=110.0+/-2.0, [m/H]=0.00+/-0.25, ccf=0.863, SNRe=36.6, R=m

The most noteworthy feature of the first observation was the presence of a double peak in the correlation function despite the phase being near zero, which we initially treated with caution due to the possibility of its being mere noise. We decided that we needed another exposure near one of the quadratures (phase at 0.25 or 0.75) to draw a conclusion.

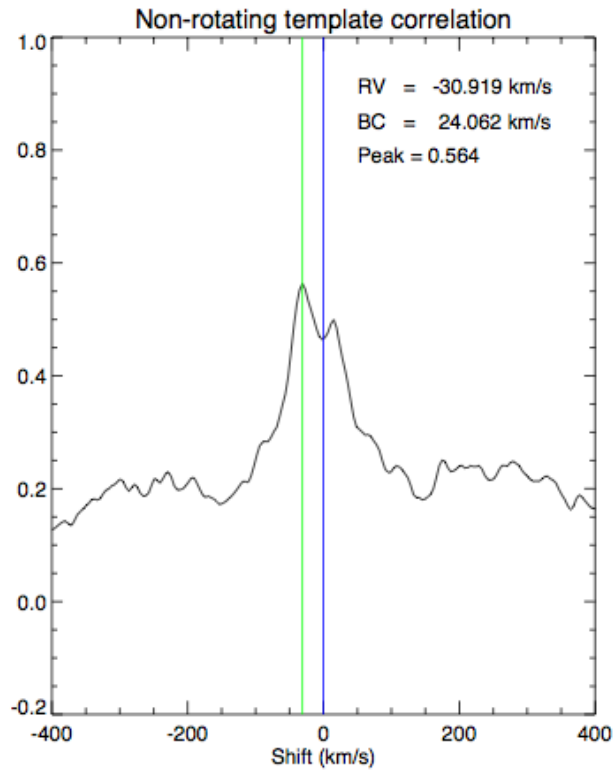


Fig. CCF for EP202094740 on first night

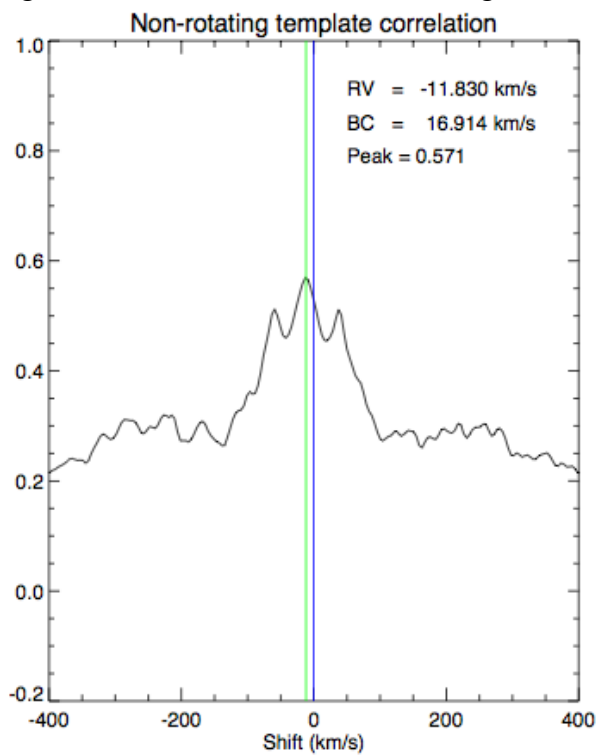
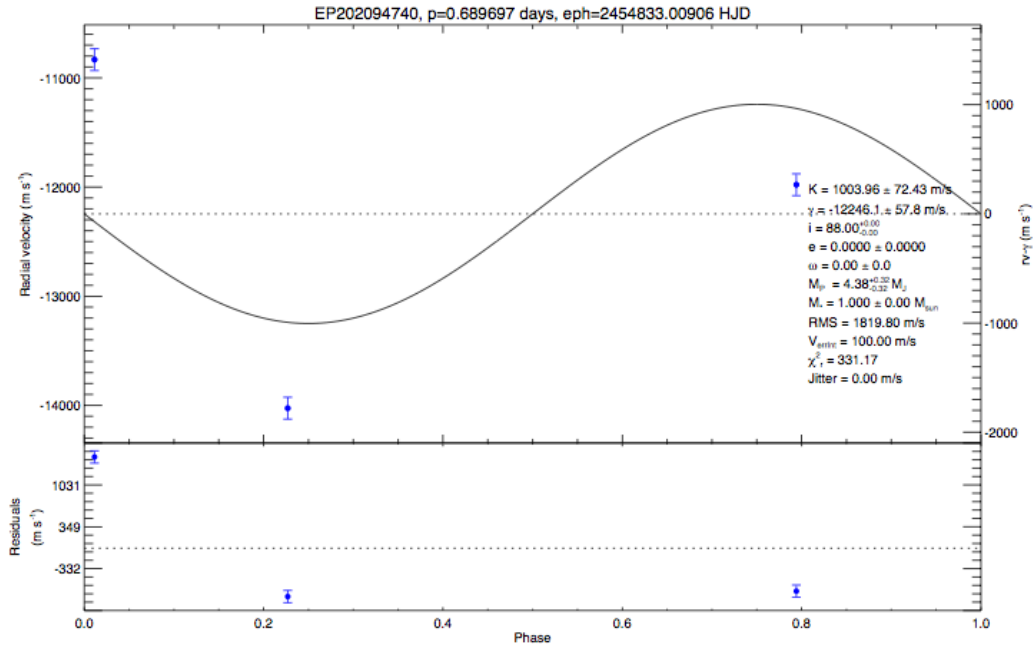


Fig. CCF for EP202094740 on second night; the third one showed a very similar pattern.

Interestingly, the second and third observations show three peaks as opposed to the two in the first. There was some variation in the radial velocities and a high chi-squared value (331). Due to the triple-lined second observation being near quadrature, we infer that the system is a hierarchical triple system, in which a binary star system is bound to another star. We consider this system irrelevant for our purposes and determined not to observe it again.



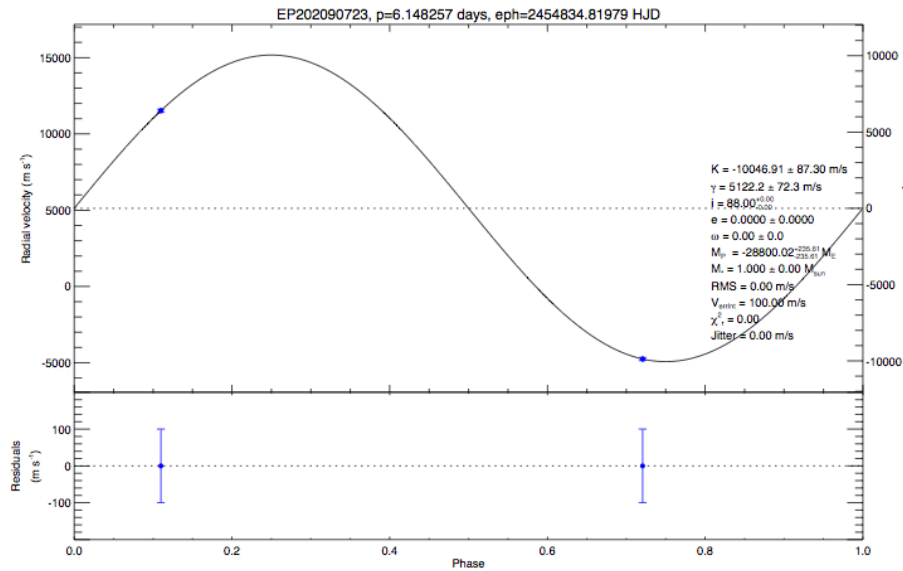
EP202090723

This is another case of a target out of phase with the photometric ephemeris. The correlation function from the first observation revealed a noticeable bump on left, so we tried again near the 0.75 quadrature. The bulge had shifted to the red side in the second observation, and we observed a velocity change. So there appears to be a companion star which is not responsible for the transit-like light curve, unless the photometric ephemeris is wrong.

EP202090723, 06:00:54.83 23:56:18.90, $V=11.0$, $PM=4.7$, $J-K=0.27$, $Period=6.1$

2014-11-07 TRES, $pha=347.11$, $RV=11.520$, $T_{eff}=6000 \pm 125$,
 $\log(g)=4.00 \pm 0.25$, $V_{rot}=20.0 \pm 2.0$, $[m/H]=0.00 \pm 0.25$,
 $ccf=0.886$, $SNRe=34.5$, $R=m$

2014-11-17 TRES, $pha=348.72$, $RV=-4.755$, $T_{eff}=6500 \pm 125$,
 $\log(g)=4.00 \pm 0.25$, $V_{rot}=25.0 \pm 2.0$, $[m/H]=0.00 \pm 0.25$,
 $ccf=0.934$, $SNRe=49.6$, $R=m$



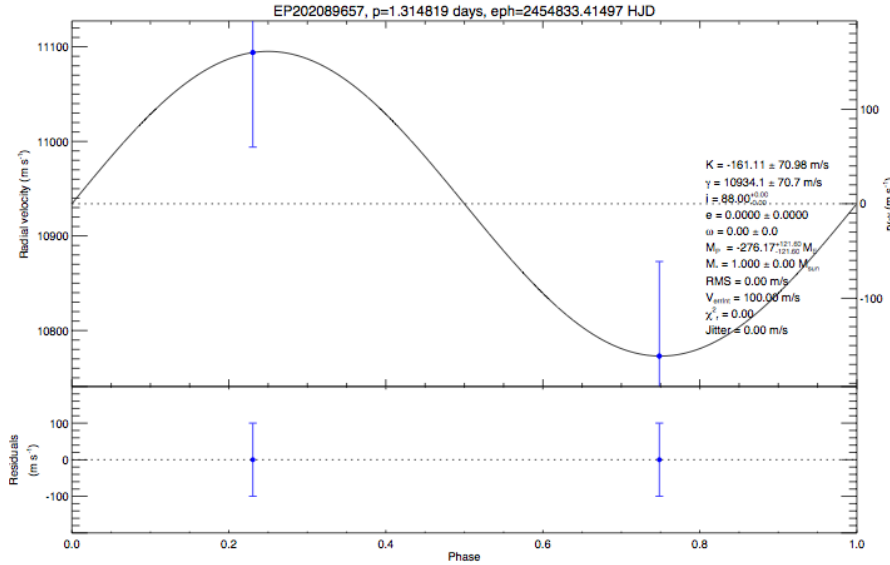
EP202089657

In either of the correlation plots from the first two observations, it was difficult to see bulges; both were clean, with symmetrical, sharp lines, and exhibited a change in radial velocity. This was another case in which the velocity change was inconsistent with the photometric ephemeris for unknown reasons.

EP202089657, 06:05:48.85 23:29:04.30, V=11.6, PM=8.0, J-K=0.31, Period=1.3

2014-11-07 TRES, pha=1624.23, RV=11.094, Teff=6500+/-125, log(g)=4.50+/-0.25, Vrot=6.0+/-2.0, [m/H]=0.00+/-0.25, ccf=0.942, SNRe=32.6, R=m

2014-11-17 TRES, pha=1631.75, RV=10.773, Teff=6500+/-125, log(g)=4.50+/-0.25, Vrot=4.0+/-2.0, [m/H]=0.00+/-0.25, ccf=0.972, SNRe=51.0, R=m



EP202087156

EP202087156, 06:24:07.07 14:46:17.30, V=12.3, PM=4.4, J-K=0.27, Period=0.9

2014-11-08 TRES, pha=2255.21, RV=26.710, Teff=6000+/-125, log(g)=2.00+/-0.25, Vrot=35.0+/-2.0, [m/H]=0.00+/-0.25, ccf=0.798, SNRe=30.1, R=m

2014-11-16 TRES, pha=2263.85, RV=27.588, Teff=6000+/-125, log(g)=2.00+/-0.25, Vrot=35.0+/-2.0, [m/H]=0.00+/-0.25, ccf=0.790, SNRe=29.5, R=m

2014-11-17 TRES, pha=2264.74, RV=27.119, Teff=6750+/-125, log(g)=3.00+/-0.25, Vrot=35.0+/-2.0, [m/H]=0.00+/-0.25, ccf=0.813, SNRe=35.8, R=m

In the first observation, we saw a bump on the right and resolved to observe at the opposite quadrature. The bulge in the correlation function peak then switched to the left for the next observation, and in the third observation the peak was roughly symmetrical.

This was a puzzling candidate due to the contradictory elements in the analysis. One way to interpret the data is to note the low gravity ($\log(g) = 2$, implying evolution or a giant star) and strong interstellar sodium D lines, and the line broadening implying a Sun-like radius. The very short period indicated by the data would require the secondary to be orbiting within the radius of the primary, which makes no sense.

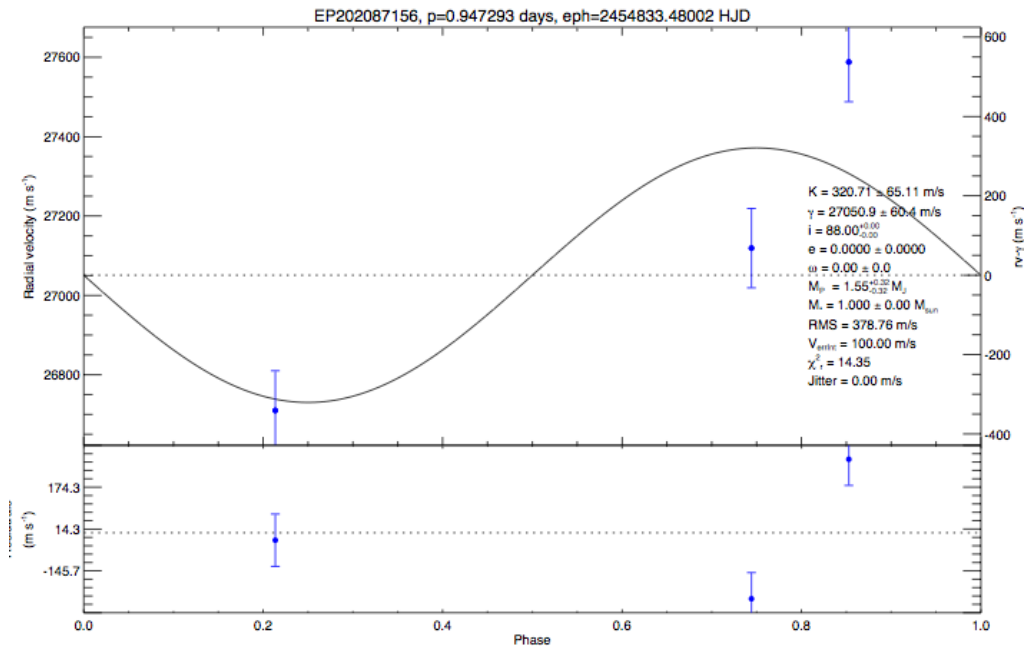
To explain this logic further, in these systems we made two general assumptions: the first was that due to tidal motions, the axes of both objects would be oriented perpendicular to the orbital plane, resulting in the rotational and orbital inclinations being equal. Second, we assumed that the orbital period and rotational period would be synchronized given that the period was sufficiently short and that the orbits were close enough to being

circular. Furthermore, we approximate the inclination as being 90 degrees in an edge-on system. Thus,

$$V \cdot \sin(i) = (2\pi R / P_{\text{rot}}) \sin(i)$$

However, the real measurements of $V \cdot \sin(i)$ and for the orbital period of the system give a primary radius value smaller than that of the Sun. Hence, according to this calculation the star cannot be a giant, contradicting what was inferred from the low surface gravity measurement.

We concluded that this candidate was not relevant for our purposes, so we decided to discard it and ascribe its anomalous characteristics to some other phenomenon in the system, such as the presence of multiple objects in the system, as in a blend with an eclipsing binary.



We see from the data here, most directly from the mass values indicated on the phase plots, that none of the observed systems are planetary.

Discussion and Conclusions

We conclude from the analysis of the photometric and spectroscopic data taken by K2 and TRES that the majority of the targets in this set are revealed to be eclipsing binary systems and other false positives. We speculate that one reason for the preponderance of false positives in this set is that during Campaign Zero, the period during which these data were taken, K2 was oriented close to the Milky Way, negatively affecting its photometric precision and increasing the number of giants and hot stars in the field. The calculations and processes described in this paper were done under the assumption that the secondary objects would be planets, but they are valid for stars as well since the physics describing both types of systems are largely the same.

It would be interesting to see what results the next K2 campaign yields and whether we will see more planetary systems in subsequent runs. Next steps would be to

look for planets with conditions similar to those on Earth – for example, densities indicating a rocky constitution, an earth-like surface gravity, and atmospheres and temperatures capable of sustaining life. However, TRES is not at present capable of probing orbits of such targets.

References

Beatty, T. G. et al. “The Mass and Radius of the Unseen M Dwarf Companion in the Single-Lined Eclipsing Binary HAT-TR-205-013”. *APJ* 663:573-582, 2007 July 1.

Faigler, S., et al. “Seven New Binaries Discovered in the Kepler Light Curves Through the BEER Method Confirmed by Radial-Velocity Observations”. *APJ* 746:185 (9pp), 2012 February 20.

Eastman, Jason. EXOFAST. Accessed November 2014.

Ribas, Ignas. “Masses and Radii of Low-Mass Stars: Theory vs. Observations.” Nov. 2005. [arXiv:astro-ph/0511431](https://arxiv.org/abs/astro-ph/0511431)

Thanks

David Latham, Guillermo Torres, Andrew Vanderburg, Allyson Bieryla, TRES staff (Gilbert Esquerdo, Perry Berlind, and Mike Calkins), Jason Eastman, Charlie Conroy, Astronomy 98